Toxicology and Applied Pharmacology 479 (2023) 116733

Contents lists available at ScienceDirect

Toxicology and Applied Pharmacology

journal homepage: www.elsevier.com/locate/taap

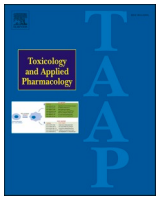

Towards translating in vitro measures of thyroid hormone system disruption to in vivo responses in the pregnant rat via a biologically based dose response (BBDR) model

Jeffrey Fisher [a,*], Conrad Housand [b], David Mattie [c], Andy Nong [a], Marjory Moreau [a], Mary Gilbert [d]

[a] ScitoVation LLC, RTP, NC, United States of America
[b] Magnolia Sciences, Winter Springs, FL, United States of America
[c] AFRL/711 HPW/RHBAF, WPAFB, OH, United States of America
[d] Office of Research and Development, Center for Public Health and Environmental Assessment, US EPA, RTP, NC, United States of America

ARTICLE INFO

Editor: Lawrence Lash

Keywords:
NAMs
HPT axis Model
PBPK
Perchlorate
Thyroid Hormones
TSH

ABSTRACT

Despite the number of in vitro assays that have been recently developed to identify chemicals that interfere with the hypothalamic-pituitary-thyroid axis (HPT), the translation of those in vitro results into in vivo responses (in vitro to in vivo extrapolation, IVIVE) has received limited attention from the modeling community. To help advance this field a steady state biologically based dose response (BBDR) model for the HPT axis was constructed for the pregnant rat on gestation day (GD) 20. The BBDR HPT axis model predicts plasma levels of thyroid stimulating hormone (TSH) and the thyroid hormones, thyroxine (T4) and triiodothyronine (T3). Thyroid hormones are important for normal growth and development of the fetus. Perchlorate, a potent inhibitor of thyroidal uptake of iodide by the sodium iodide symporter (NIS) protein, was used as a case study for the BBDR HPT axis model. The inhibitory blocking of the NIS by perchlorate was associated with dose-dependent steady state decreases in thyroid hormone production in the thyroid gland. The BBDR HPT axis model predictions for TSH, T3, and T4 plasma concentrations in pregnant Sprague Dawley (SD) rats were within 2-fold of observations for drinking water perchlorate exposures ranging from 10 to 30,000 μg/kg/d. In Long Evans (LE) pregnant rats, for both control and perchlorate drinking water exposures, ranging from 85 to 82,000 μg/kg/d, plasma thyroid hormone and TSH concentrations were predicted within 2 to 3.4- fold of observations. This BBDR HPT axis model provides a successful IVIVE template for thyroid hormone disruption in pregnant rats.

1. Introduction

The hypothalamic-pituitary-thyroid (HPT) axis is a well-studied component of the endocrine system. Disturbances in the HPT axis, most prominently hypothyroidism, represent a significant public health concern, especially in the developing fetus (Gilbert et al., 2020). Drugs, chemicals, and dietary deficiencies can disrupt thyroid hormone regulation and signaling at several distinct target sites (Zoeller, 2007). These include targets involved with thyroid hormone synthesis and its distribution, metabolism, and elimination (Miller et al., 2009; Zoeller, 2007). The complexity of the thyroid system coupled with its necessity for normal growth and development has led to the emergence of several new approach methodologies (NAMs) targeting various aspects of the HPT axis. These NAMs include in vitro screening tools to evaluate thyroid peroxidase (Friedman et al., 2016), thyroid hormone metabolism (Olker et al., 2019), and the sodium iodide symporter (NIS) protein (Wang et al., 2018).

The overall objective of this study was to construct a fit-for-purpose BBDR HPT axis model in late pregnancy of the rodent with the eventual capability of predicting thyroid hormone disruption by different molecular initiating events (MIEs). As a case study, we chose the MIE event blockage of thyroidal iodide uptake at the NIS protein. Perchlorate was selected for the case study because it is a well-studied potent inhibitor of the NIS protein. The ability of perchlorate to inhibit the uptake of iodide into thyroid cells has been known since the early 1960s (Wolff and Walrey, 1963). The molecular identity of the NIS protein, responsible for

* Corresponding author.
E-mail address: jfisher@scitovation.com (J. Fisher).

https://doi.org/10.1016/j.taap.2023.116733
Received 10 September 2023; Received in revised form 18 October 2023; Accepted 19 October 2023
Available online 20 October 2023

active uptake of iodide, was first characterized in 1996 in the rat (Dai et al., 1996). Several perchlorate Ki values have been determined using in vitro thyroid cell systems (see Table 1) with Ki values ranging from 17.3 to 149.18 μg/L. These Ki values represent the calculated concentrations of perchlorate that are associated with a 50% inhibition in radioactive iodide uptake in thyroid cells. Perchlorate Radioactive Iodide Uptake (RAIU) inhibition studies in vivo have been conducted in adult rats (Merrill et al., 2003), pregnant rats (Clewell et al., 2003) and humans (Merrill et al., 2005) by measuring radioactive iodide in the thyroid glands. For adult rats, Merrill et al. (2003) employed an in vivo PBPK model fitted Ki value of 180 μg/L to describe RAIU inhibition by perchlorate. For humans Merrill et al. (2005), derived an in vivo PBPK model fitted Ki value of 160 μg/L to describe the RAIU inhibition by perchlorate. Two in vivo BBDR HPT axis models for perchlorate, one in the adult rat (McLanahan et al., 2008), and another in the pregnant human (Lumen et al., 2013) set the Ki values for perchlorate equal to Kosugi et al. (1996) reported Ki value of 149.18 μg/L.

A perchlorate RAIU PBPK model for the pregnant rat (Clewell et al., 2003) was of interest and used in development of the current pregnant rat BBDR HPT axis model for perchlorate. Clewell et al. (2003) set Ki value of 100 μg/L that was intermediate to reported Ki values by Wolff and Walrey (1963) and Kosugi et al., 1996 (see Table 1). There are several important model parameters obtained from the literature to create the HPT axis model for the pregnant rat, beyond the chemical specific Ki value. These model parameters and the model equations shown in the Methods and Supplementary Tables provide a foundation for those interested in the development of a relatively simple pharmacodynamic model for the thyroid system.

Table 1
Reported Ki values for the inhibition of radioiodide uptake into the thyroid gland by perchlorate and Ki values used in RAIU PBPK and BBDR HPT axis models for perchlorate.

Ki for perchlorate	In vitro system	Reference
0.4 μM or 39.78 μg/L	Sheep thyroid slice	(Wolff and Walrey, 1963)
1.5 μM or 149.18 μg/L	Chinese Hamster Ovary Cell line transfected NIS gene from FRTL-5 (rat) thyroid cell line	(Kosugi et al., 1996)
0.59 μM or 58.67 μg/L	Reanalysis of Kosugi et al., 1996 data	(Schlosser, 2016)
0.448 μM or 44.55 μg/L ($KClO_4$) 0.866 μM or 86.12 μg/L ($NaClO_4$)	hNIS-HEK293T-EPA cell line	(Hallinger et al., 2017)
0.1698 μM or 17.69 μg/L ($KClO_4$) 0.1738 μM 17.28 μg/L ($NaClO_4$)	FRTL-5 rat cell line	(Buckalew et al., 2020)
1.45 μM or 144.20 μg/L	PCCL3 rat follicular thyroid cell line	(Rolland et al., 2023) (Society of Toxicology poster)
180. μg/L	RAIU PBPK model, adult rat, based on Kosugi et al. (1996), fit to in vivo data	(Merrill et al., 2003)
160. μg/L		(Merrill et al., 2005)
100. μg/L		(Clewell et al., 2003)
149.18 μg/L	RAIU PBPK model, adult human, based on Kosugi et al. (1996), fit to in vivo data	(McLanahan et al., 2008)
149.18 μg/L		(Lumen et al., 2013)
	RAIU PBPK model, pregnant rat, set to value between Kosugi et al. (1996) and Wolff and Walrey (1963)	
	BBDR HPT axis model, adult rat, set to Kosurgi et al. (1996)	
	BBDR HPT axis model, pregnant human, set to Kosurgi et al. (1996)	

2. Methods

2.1. Pregnant rat perchlorate studies

The following perchlorate drinking water studies using pregnant rats (Clewell et al., 2003; Gilbert, 2023; Mahle et al., 2003) provided plasma levels of perchlorate. Clewell et al. (2003) conducted perchlorate drinking water pharmacokinetic studies at several doses with Sprague Dawley (SD) pregnant rats from GD2 to GD20. Mahle et al. (2003) performed a drinking water perchlorate study from GD2 to GD20 with a single dose to examine in utero and post-natal pharmacokinetics of perchlorate in SD rats. Gilbert (2023) measured perchlorate plasma levels on GD16 and GD20 in Long-Evans (LE) pregnant rats exposed to several doses of perchlorate from GD6 to GD20 (Gilbert et al., 2022). In all studies, animals were euthanized on GD20.

The following perchlorate drinking water studies using pregnant rats (Gilbert et al., 2022; Mahle et al., 2003; York et al., 2003) provided plasma thyroid hormones and TSH. York reported serum levels of T3, T4 and TSH in SD dams and fetuses on GD21 for exposure to several doses of perchlorate from GD0 to GD21. Mahle et al. (2003) measured thyroid hormones and TSH in GD20 in the dam and fetus in conjunction with perchlorate exposure. Gilbert et al. (2022) measured serum thyroid hormones in GD16 and GD20 LE rats (dam and fetus) following perchlorate exposure to several dose groups that began on GD6.

2.2. Construction of a perchlorate PBPK model

A PBPK model for the pregnant rat and her fetal progeny was constructed (Fig. 1) based on prior rat pregnancy models (Clewell et al., 2003; Yoon et al., 2009) and created new equations from ontogeny data found in the literature. The maturation equations and references are found in Supplementary Tables S1 and S2. This PBPK model describes the ontogeny of the physiology in the dam and the fetal litter from the day of impregnation (GD0) to late-term pregnancy (GD20). Ninety five percent of administered perchlorate is cleared in urine by 24 h (Merrill et al., 2003). However, perchlorate's urinary clearance in the rat is less than the glomerular filtration rate (Merrill et al., 2003). As an anion, perchlorate may be subject to transport by a protein transporter in the kidney slowing its excretion in urine. There is also evidence of low capacity and high affinity binding of perchlorate with plasma serum proteins (Campbell et al., 2004; Rivard, 2007). At low perchlorate concentrations, the serum protein binding appears substantial and binding decreases significantly with higher perchlorate concentrations. Table S3 contains perchlorate specific model parameters for the pregnant rat PBPK model. To describe the pharmacokinetics of perchlorate across wide ranges of doses (10 to 30,000 μg/kg/day in SD rats and 85 to 82,000 μg/kg/day in LE rats), urinary excretion and fraction bound to plasma protein were visually fitted to perchlorate plasma concentrations across doses and strains of pregnant rats. It is unknown if the serum binding profiles for perchlorate are the same or different for SD and LE strains. For modeling purposes, modest differences were assumed. Only serum protein binding and urinary clearance were adjusted for the perchlorate PBPK model.

Simulation models were run for 484 h to reach steady state conditions using Magnolia 1.3.11 Beta (https://www.magnoliasci.com/). Simulations assumed a 12-h drinking schedule each day for perchlorate in a similar manner as Clewell et al. (2003).

2.3. Construction of thyroid hormone and thyrotropin (TSH) maternal compartmental models Fig. 2)

The HPT feedback regulation is complex at the biochemical and molecular biology levels and involves the thyroid and pituitary glands, as well as central control by the hypothalamus in the brain (Fekete and Lechan, 2007; Fliers et al., 2006; Rodríguez-Rodríguez et al., 2019). Disruption of thyroid hormone homeostasis can occur in the gland itself,

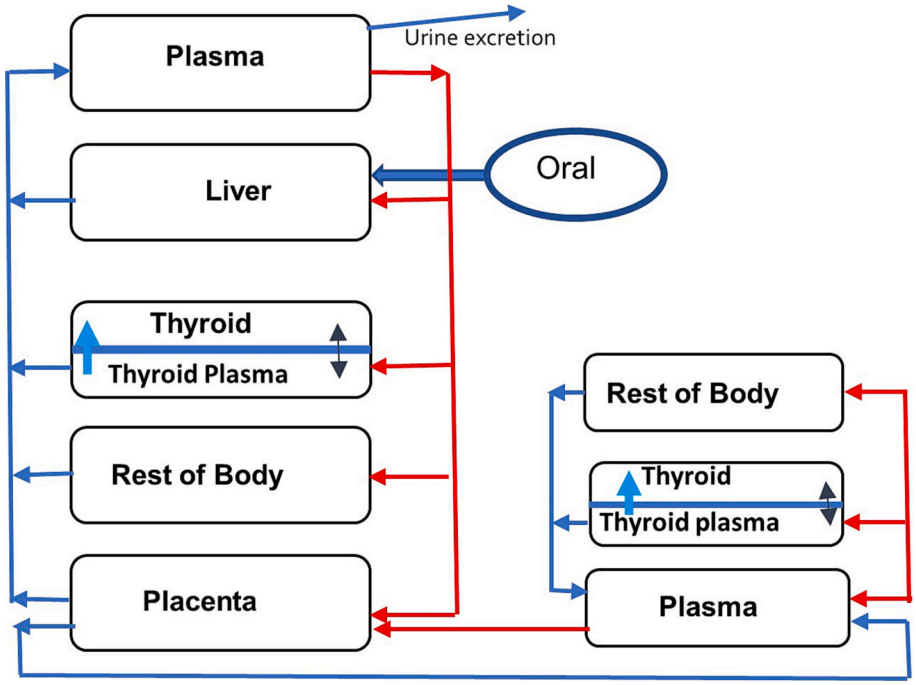

Fig. 1. Schematic of a pregnant rat PBPK model for perchlorate. Model parameters are found in the Supplementary Tables S1, S2, and S3 for age dependent maturation of the fetus and dam during gestation. The model code is found in supplementary.

in the periphery with local hormone transport and metabolism in target organs including the brain. Thyroid hormones are secreted from the thyroid gland (T4 and T3). Most serum T3 is produced, however, from hepatic deiodination of free T4. In the hypothalamus free T4 is metabolized to T3. It is this T3 that is responsible for the regulation (inhibition) of thyrotropin-releasing hormone (TRH) and the control of TSH secretion from the pituitary gland into the blood supply (Fekete and Lechan, 2007; Fliers et al., 2006; Rodríguez-Rodríguez et al., 2019). Secreted TSH travels in the blood supply to the thyroid gland, where TSH upregulates (induces) the amount of transporter protein (NIS) to sequester iodide from the blood for use in the synthesis of thyroid hormones. This initial step for TSH regulation of thyroid hormone production is governed by the binding of TSH to receptors on the gland (thyrotropin receptor, TSHR) (Jing and Zhang, 2022). Activation of TSHR causes a cascade of reactions to increase the production and secretion of thyroid hormones.

Unlike a more complex HPT axis modeling approach used to describe the T4-TSH feedback system for the adult rat (McLanahan et al., 2008), a simpler approach was constructed for the feedback system. Like McLanahan et al. (2008), one compartmental models were used for T4, T3, and TSH to represent the maternal-fetal unit. No iodide was accounted for in the current model, nor was a thyroid gland explicitly described.

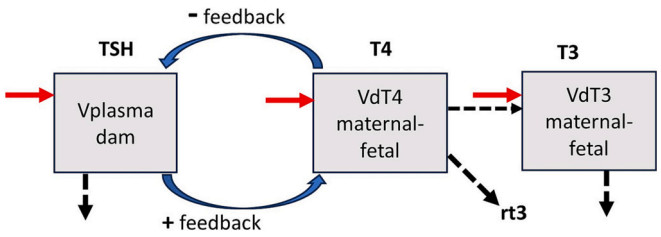

Fig. 2. Schematic of HPT axis model for the pregnant rat. Model parameters and equations are found in the Methods section. The model code is found in supplementary. The solid arrows represent production of TSH, T4, and T3, and the dotted arrows represent metabolism for TSH, T4, and T3. The volume of distribution for T4 (VdT4) and T3 (VdT3) represent both the dam and fetus and for TSH, maternal plasma volume (Vdamplas_kg).

The negative feedback (T4 affecting TSH production) and positive feedback (TSH affecting T4 production) were calibrated at steady state plasma levels of total T4 and TSH, including inhibition of T4 production by perchlorate.

The HPT axis equations (Goede, 2022; Goede et al., 2014) represent simple mathematical depictions of the HPT axis. TSH is produced at a zero-order rate, distributes within the plasma volume, and is metabolized in the plasma. TSH production is decreased if plasma T4 concentrations are high and vice versa if plasma T4 concentrations are low. In our case, using plasma concentrations of total T4 (bound and unbound in plasma) provided a fit-for-purpose methodology for the negative feedback, like McLanahan et al. (2008). Total T4 production is controlled by TSH plasma concentrations. In the presence of perchlorate, the NIS protein on the basolateral side of the thyroid gland is upregulated by TSH resulting in an assumed proportional increase in T4 production because of increased availability of iodide. In concert with TSH upregulation of NIS is an opposing MIE by perchlorate - the blocking effect of perchlorate on the NIS protein sequestration of iodide (Yu et al., 2002). The result is a dose-dependent decrease in T4 and T3 production in the gland and a decrease in serum T4 concentrations as demonstrated by Yu et al. (2002). The blocking effect of perchlorate at high exposures appears incomplete. In this model, T4 metabolism occurs within the T4 volume of distribution. The thyroidal production of T3 is assumed to be 10% of the T4 thyroidal production rate based on the lactating rat model (Fisher et al., 2013), which was derived from adjusting experimental estimates of about 20% (De Escobar et al., 1990) in the rat. The primary source of T3 is derived from deiodination of T4 to T3 and reverse T3 (inactive, rT3). Fifty percent of metabolized T4 is assumed to be converted to rT3 (Lumen et al., 2013).

2.4. Evaluation and selection of NIS Ki

Initially a Ki of 100 μg/L was selected to evaluate the model predictions of plasma concentrations of T4 based on an in vivo RAIU model for the pregnant rat (Clewell et al., 2003). This Ki value was retained in the final BBDR HPT axis model for the pregnant rat. The impact of using a range of Ki values (Table 1) on predicted T4 plasma concentrations is

considered in the Discussion section.

2.5. Key model equations

The units for the thyroid hormones and TSH equations are nM, nmole/h and L/h. Tables 2 and 3 provide the HPT model parameter references, units, and values.

2.5.1. Thyroid stimulating hormone (TSH)

TSH (RTSH, nmole/h) was described with a TSH basal synthesis rate (RTSH*syn*) that was adjusted based on the plasma concentration of T4 (negative feedback, RTSH*inhib*). Clearance of TSH occurred in the plasma (RTSH*met*).

1) $RTSH\left(\frac{nmole}{hr}\right) = RTSHsyn - RTSHinhib - RTSHmet$ (Goede, 2022; Goede et al., 2014)

RTSH*syn* = production rate of TSH (nmole/h).
RTSHmet = metabolic rate of TSH (nmole/h)

2) $RTSHinhib\left(\frac{nmole}{hr}\right) = RTSHsyn^{*}\left(\frac{Cplasma_{T4}}{(1+Cplasma_{T4})}\right)$, T4 negative feedback (Goede, 2022)

$Cplasma_{T4}$ = plasma concentration of total T4 (nmole/L).

2.5.2. Thyroxine (T4)

The description of T4 (RT4, nmole/h) is more complicated than TSH. The basal synthesis and secretion rate of T4 ($Emaxb_{T4}$, nmole/h) is adjusted by plasma concentrations of TSH (positive feedback, Eq. 3). T4 is metabolized (deiodinated) to T3 and rT3. Perchlorate exposures upregulate the NIS protein (NISind), which results in increased sequestration of iodide and synthesis and production of T4. NIS gene expression was measured in pregnant LE rats (Gilbert et al., 2022) and assumed to be similar in SD pregnant rats. Gene expression (fold increase) and protein abundance (fold increase) were assumed to be equal.

Table 2
Model parameters and references used in the HPT axis model for the pregnant rat.

Model Parameter	Value Used in Model	Reference, species, reported value
TSH synthesis, RTSH*syn*	0.2*	(D'angelo et al., 1976), euthyroid female Sprague-Dawley (0.11 nmole/h)
TSH metabolism Clearance, TSH_CL	0.03*	(Griessen and Lemarchandberaud, 1973), male Wistar rats (0.048, L/h)
TSH Volume of distribution, Vplasma	Ontogeny equation	(Nadel et al., 1988), age dependent equation for plasma, L, in supplementary Table S1, pregnant rat
T4 production, Emax_T4b	0.2*	(Lu and Anderson, 1994), 0.065 nmole/h pregnant rat, maximal rate 4 μg/day or 0.2 nmole/h
T4 NIS induction Fold increase, NISind	dose dependent	(Gilbert et al., 2022), 1 to 6.28, pregnant rat, unitless, values in Table 3
T4 concentration, Half maximal TSH production, EC50	0.20	(McLanahan et al., 2008), nmole/L
Perchlorate inhibition constant, Ki,	100	(Clewell et al., 2003), μg/L
T4 volume of distribution, Vdf	0.21	(Lu and Anderson, 1994), fraction of body weight, pregnant rat near term, unitless
T4 metabolism, KelT4	0.048	(Lu and Anderson, 1994), /h, first order, converted to clearance, L/h, pregnant rat
T3 metabolism, clearance, CLT3,	0.08	(Versloot et al., 1998), L/hr/kg, pregnant rat
T3 volume of distribution, VdT3c	0.67	(Versloot et al., 1998), fraction of body weight, pregnant rat

* Fitted.

Table 3
NIS gene expression fold increases for perchlorate dose groups.

Dose SD rats**	NISind	Dose LE rats*	NISind
10	1	85	1.09
100	1	2200	5.98
1000	2	23,250	6.28
30,000	6.28	82,000	6.28

*Measured, Gilbert et al., 2022. **Fit.

Upregulation of NIS protein was suspected in SD rats when perchlorate levels in the thyroid gland were increased when the SD rats were placed on drinking water containing perchlorate for 14 days (Merrill et al., 2003). In addition, thyroidal iodide is blocked, in a concentration dependent manner, by perchlorate at the NIS protein resulting in a decrease in the synthesis and secretion of T4. With very high levels of perchlorate, the plasma levels of T4 were not completely depleted indicating that blocking NIS is not 100% complete. Reduced T4 production was observed in NIS knock-out mice suggesting that the thyroid gland has some ability to function without the NIS symporter protein (Ferrandino et al. 2017). From a simulation perspective, it appears that this pathway may be under the influence of TSH (see Discussion). Therefore, to predict the serum thyroid hormones and TSH at very high perchlorate exposures, a slow perchlorate- independent and TSH-dependent residual production rate of T4 (Eq. 5, Residual) was necessary. A residual production rate of T4 was calculated by dividing the TSH influenced NIS upregulated rate of production of T4 ($Emaxb_{T4}$*-*NISind*) by a value of 20. A value of 20 was selected after various visual fitting attempts using larger and smaller values to describe T4 production at high levels of serum perchlorate. At low exposures of perchlorate, the term Residual had negligible influence as implemented in the Eq. 5 below.

3)

$$RT4\left(\frac{nmole}{hr}\right) = Emax_{T4}{}^{*}\left(\frac{Cplasma_{TSH}}{EC50 + Cplasma_{TSH}}\right) - RT4met + Residual$$

4)

$$Emax_{T4} = Emaxb_{T4}{}^{*}NISind - Emaxb_{T4}{}^{*}NISind^{*}\left(\frac{Cplasma_{clo4}}{Cplasma_{clo4} + Ki}\right)$$

RT4met = Metabolic rate for T4 (nmole/h).
$Cplasma_{TSH}$ = concentration of TSH in plasma (nmole/h).
EC50 = plasma concentration of T4 at half maximal TSH production (nmole/L).
$Emaxb_{t4}$ = basal rate of T4 production (nmole/L).
NISind = fold increase in NIS (*Slc5a5 transcript*) (Gilbert et al., 2022).
$Cplasma_{clo4}$ = plasma unbound concentration of perchlorate (μg/L).
Ki = inhibition affinity constant for perchlorate and NIS protein (μg/L)

5)

$$Residual\left(\frac{nmole}{hr}\right) = \frac{Emaxb_{t4}{}^{*}NISind}{20}$$

2.5.3. Triiodothyronine (T3)

T3 (RT3, nmole/h) is formed from metabolism of T4 and to a limited degree from synthesis and secretion from the thyroid gland. T3 is metabolized to diiodothyronine (T2). Hepatic metabolism (deiodina-

tion) of T4 yields T3 (50% RT4*met*) and reverse T3, rT3 (50%). The thyroidal production rate of T3 was set to 10% of the rate of thyroidal production of T4 (RT3*thyroid*).

6)

$$RT3\left(\frac{nmole}{hr}\right) = 0.5*RT4met + 0.1*RT3thyroid - RT3met$$

RT3*met* = rate of metabolism of T3 (nmole/h).

3. Results

For euthyroid (control) SD rats, the concentration of total T4 in plasma provided the best surrogate for mimicking the negative feedback that occurs in the brain (Eq. 2). This outcome is consistent with previous modeling efforts in the adult rat reported in McLanahan et al. (2008). The next step was to provide a set of HPT model parameters for control SD rats that would predict plasma levels of TSH and thyroid hormones within 2-fold based on World Health Organization recommendations for the performance of PBPK models (WHO, 2010).

3.1. Control pregnant rats

Exploratory manual simulations were necessary and conducted by adjusting model parameters in Table 2 to fit control thyroid hormones and TSH for the SD rat. From these simulations, the final calibration of model parameters summarized in Table 2 involved increasing the literature reported TSH production rates from 0.11 to 0.20 and T4 production rates from 0.065 to 0.20 nmole/h, while the reported TSH plasma clearance (TSH metabolism) was decreased from a starting value of 0.048 to 0.03 L/h. These steps were carried out sequentially. Visual inspections of plasma T4, T3, and TSH concentrations were compared to experimental values after each parameter change. Other model parameters were not changed. These adjustments provided euthyroid model predictions for plasma total T4, total T3, and TSH within the targeted 2-fold of measured levels in the SD rat (Fig. 3a, 3b, 3c). Using the calibrated SD rat HPT model, the predicted euthyroid plasma TSH levels in LE pregnant rats were overpredicted by 2.6-fold in control rats (Fig. 4b), while T4 and T3 predictions agreed with observations (Fig. 4a, 4c).

For the negative feedback (T4 ➔TSH) and positive feedback (TSH➔T4) loops to provide reasonable baseline (euthyroid) predictions of plasma T4, T3, and TSH concentrations, the production rates of TSH (RTSHsyn) and T4 (Emax_T4b) could not vary much from what was used. In this sense, these parameters are sensitive, and the system is tightly controlled. The experimentally determined values for the TSH and T4 production rates were important for calibration of the thyroid system of equations, as were their volumes of distribution, and rates of clearance via metabolism. We attempted to retain the whole body calculated HPT axis model parameters, derived from independent studies, but adjusted a few of the HPT axis parameters to enable agreement between model predictions of measured plasma concentrations of TSH and thyroid hormones.

3.2. Pregnant rats exposed to perchlorate in drinking water

Table 4 provides a comparison of model predicted and observed concentrations of perchlorate in plasma of pregnant SD and LE rats on GD20. The plasma levels of perchlorate were adequately predicted (with a factor of 2) for SD and LE rats for all dose groups. There was a trend to underpredict the perchlorate plasma concentrations in the LE rats.

The primary perchlorate studies reporting dose-dependent perturbations in pregnant SD rat serum thyroid hormones and TSH were York et al. (2003) and Mahle et al. (2003) and for LE rats, Gilbert et al. (2022).

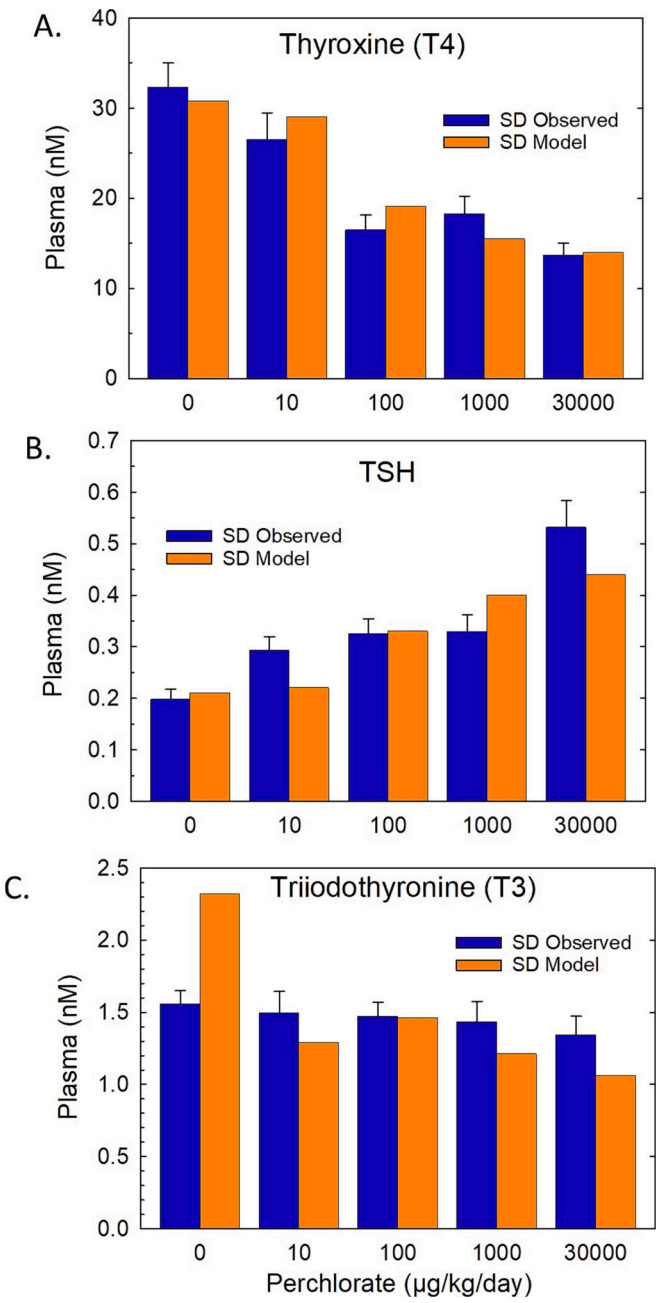

Fig. 3. a, b, c. HPT axis model predictions (second bar) versus observations (first bar with standard deviation) in Sprague Dawley pregnant rats on GD20 for plasma concentrations of thyroid hormones and TSH (a. T4, b. TSH, c. T3). Control and perchlorate exposure groups are represented. All model predictions are within 2-fold of experimental findings.

The HPT pregnant rat model was successful in predicting plasma concentrations of TSH and thyroid hormones within 2-fold for drinking water exposures that ranged from 10 to 30,000 µg/kg/day (Fig. 3a, 3b, 3c) in the SD strain. In the LE rat (Fig. 4 a, b, c), all predictions were within 2-fold except for the following: TSH concentrations were overpredicted in control and the two lowest doses of perchlorate (85 and 2200 µg/kg/d) by factors of 2.6-, 3.0- and 3.4-fold, respectively, and T4 was overpredicted by 2.3-fold in the 82,000 µg/kg/d dose group.

The range of perchlorate drinking water exposures allowed for a robust dose response evaluation of the HPT equations in the pregnant rats. T4 measured plasma concentrations ranged from 32.4 µM in control rats to 13.6 µM in pregnant SD rats exposed to 30,000 µg/kg/d of perchlorate with corresponding increases in plasma TSH concentrations

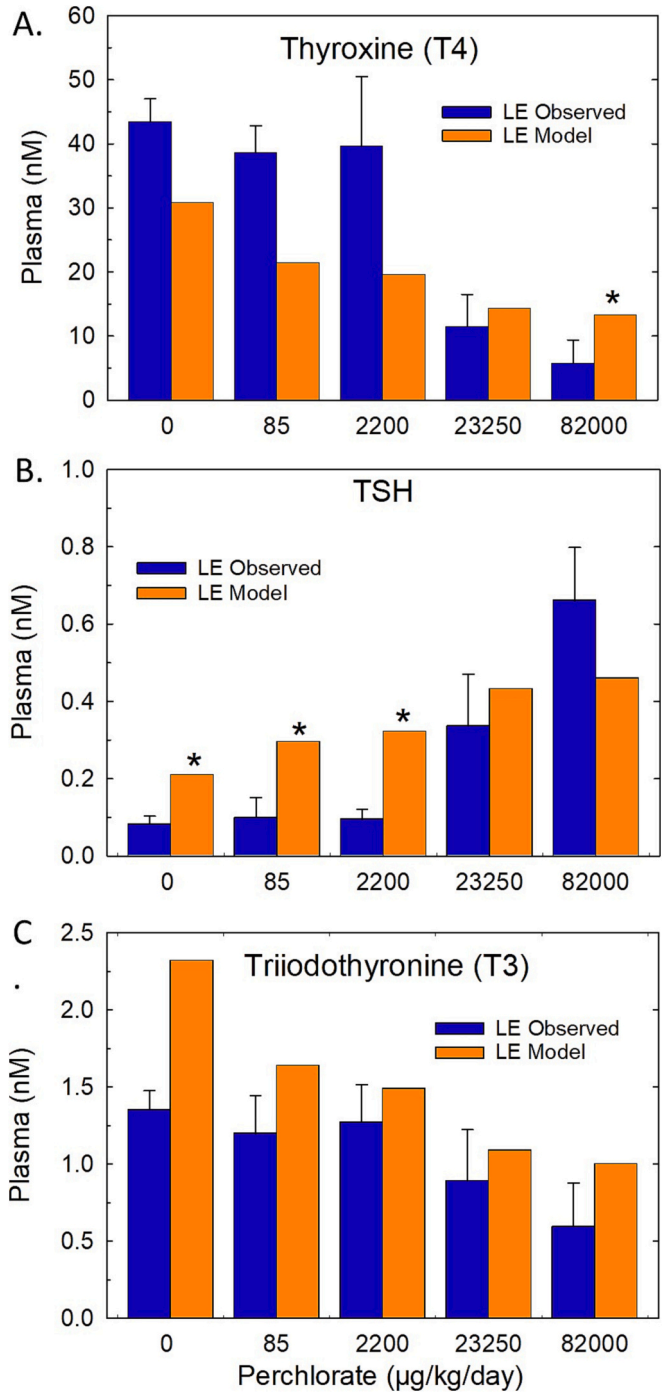

Fig. 4. a, b, c. HPT axis model predictions (second bar) versus observations (first bar with standard deviation) in Long Evans pregnant rats on GD20 for plasma concentrations of thyroid hormones and TSH (a. T4, b. TSH, c. T3). Model predictions with a asterisk sign (*) are >2-fold difference compared to observations. Control and perchlorate exposure groups are represented. All other model predictions are within 2-fold of observations.

from 0.2 to 0.53 µM. For LE rats, control T4 measured levels dropped from 43.4 in control rats to 5.75 µM in rats exposed to 82,000 µg/kg/day with corresponding increases in plasma TSH from 0.08 to 0.66 µM.

3.3. Sensitivity analysis

A limited time-dependent local sensitivity analysis was undertaken to determine the importance of the HPT model parameters shown in

Table 4
Mean measured and predicted concentrations of perchlorate in plasma of GD20 rats. Sprague Dawley rat data were taken from Clewell et al. (2003) and Mahle et al. (2003)*, and Long Evans rat data were reported in Gilbert et al. (submitted).

Sprague Dawley	10 µg/kg/day	100 µg/kg/day	1000 µg/kg/day	30,000 µg/kg/day**
Measured (µg/L)	46	116	673, 710*	
Predicted (µg/L)	48	138	699	
Long-Evans	85 µg/kg/day	2200 µg/kg/day	23,250 µg/kg/day	82,000 µg/kg/day
Measured (µg/L)	173	5252	26,961	73,278
Predicted (µg/L)	118	3656	16,251	49,080

** No measured plasma perchlorate concentrations available.

Table 2 to predict the plasma concentrations of T4. The calibrated model parameters were used with the local sensitivity analysis command (lsa). Each model parameter was increased by 0.1% of its original value while keeping all the other parameters fixed. Normalized sensitivity coefficients (NSCs) were determined using the central difference approximation to the partial derivative and normalized to both the original model parameter and model output. The normalized sensitivity coefficients

$$(\mathrm{NSC}) = \frac{O2 - O1}{O1} \times \frac{P1}{P2 - P1}$$

where O1 equals the model output with the original model parameter, O2 equals the model output with the adjusted model parameter, P1 equals the value of the original model parameter, and P2 equals the adjusted model parameter value. Parameters with absolute NSC values >0.5 were considered the most sensitive and those with values ranging from 0.2 to <0.5 were designated less sensitive. The most sensitive parameters (>|0.5|) for control pregnant rats were T4 secretion (Emax_T4b), metabolism (T4*met*), and volume of distribution (fraction of body weight) (Vdf). These same parameters were important for perchlorate exposures (10 and 30,000 µg/kg/d), with the addition of NIS (NISind) and Ki for the 30,000 µg/k/d perchlorate exposure. Other less sensitive (>|0.5| < |0.2|) model parameters included TSH production (RTSH*syn*), TSH clearance (TSH*met*), and the EC50.

4. Discussion

A successful fit-for-purpose BBDR HPT axis model for the pregnant rat was constructed to predict maternal perturbations in plasma thyroid hormones and TSH under steady state conditions for perchlorate. In this case, there were several perchlorate MIE studies for RAIU inhibition that were carried out using a variety of in vitro systems (Table 1). To understand better the implications of using the range of reported in vitro Ki values, simulations with the SD pregnant rats were carried out with Ki values ranging from 17.28 to 149.18 µg/L for perchlorate. Three perchlorate exposures representing the lowest, the highest and a mid-range were selected for the simulations (10, 1000, and 30,000 µg/kg/d). The measured mean total T4 concentrations were compared to model predictions. For the 10, 1000, and 30,000 µg/kg/d perchlorate exposures, the predicted plasma total T4 concentrations were within 3 to 13%, 3 to 57%, and 2 to 14% of measured plasma total T4 concentrations, respectively. This suggests that the current BBDR HPT axis model provided reasonable predictions within a factor of 2 (100%), using any of the reported Ki values. Eqs. 1–5 provide a framework for future MIE modeling efforts involving IVIVE. The thyroid hormone compartments can be modified to accommodate other MIEs such as hepatic metabolism of thyroid hormones or a plasma compartment to describe protein

binding of thyroid hormones. To obtain better agreements between observations and predictions for LE pregnant rats, the current model would need to be calibrated using TSH data for this strain of rat.

The selection of plasma T4 concentration in rats as a point of departure (POD) appears to be a good choice because it is a sensitive biomarker of endocrine function. Maintaining normal circulating levels of thyroid hormones is recognized as important during development. The ultimate biomarker for thyroid hormone disruption would be target tissue or cell measurements of T3 (Bianco, 2022), the physiologically active thyroid hormone. However, these measurements are rare in toxicology studies. The decisions for the selection of a POD range from using statistics to compare chemical induced reductions in plasma T4 levels with control plasma T4 levels to associating plasma T4 levels with downstream biomarkers of developmental toxicity or developmental toxicity endpoints. For hearing loss in neonatal rats (Crofton, 2004), a 50% decline in plasma T4 levels was required for an association between hearing loss and plasma T4 levels. Substantial decreases in plasma T4 levels may not be associated with dam and pup hearing loss, brain function or behavior tests (Ramhøj et al., 2022), which may suggest that the methods to identify developmental neurotoxicity are insufficient. In some cases, plasma TSH concentrations do not increase in response to a decrease in plasma total and free T4 concentrations (Hallgren et al., 2001). This was the case for dosing rats dosed with polybrominated diphenyl ethers and polychlorinated biphenyls (Hallgren et al., 2001). Dose-response relationships for thyroid mediated developmental neurotoxicity are complex, but BBDR HPT axis models provide a framework for considering in vivo dose responses based on MIEs derived from in vitro systems.

The expectations for this BBDR HPT axis model should be consistent with the recognition that this model is a simplistic description of complex processes and there are gaps in knowledge about how the HPT axis functions. For example, the ability of the thyroid gland to secrete thyroid hormones at very high levels of perchlorate exposure is not well understood. Thyroxine secretion continues even with a severe thyroglobulin mutation (Zhang et al., 2021). BBDR HPT axis models can help to understand better the functioning of the thyroid system. Thus, as more HPT axis models are used to evaluate in vitro MIE data and limited in vivo data, the utility of this methodology will be forthcoming. Extending the current BBDR HPT axis model to incorporate the fetus and earlier times in maternal pregnancy would enhance effectiveness since the fetus is the focus for neurodevelopmental deficits. The development of a human BBDR HPT axis model for the 3 trimesters of pregnancy is important and can used for IVIVE using MIE data generated from in vitro assays of human induced pluripotent stem cells (iPSCs) (Ramhøj et al., 2023) transfected cells with human proteins and receptors, and human based organoids (Deisenroth et al., 2020).

Disclaimer

This document has been subjected to review by the US Environmental Protection Agency Center for Public Health and Environmental Assessment and approved for publication. Approval does not signify that the contents reflect the views of the Agency, nor does mention of trade names or commercial products constitute endorsement or recommendation for use.

The views expressed in this article are those of the authors & do not necessarily reflect official policy or position of the U.S. Air Force, Department of Defense, nor the U.S. Government. Some of this work was prepared as part of official duties by employees of the U.S. Government. ScitoVation LLC funded, in part, this research project.

Declaration of Competing Interest

The authors declare that they have no known competing financial interests or personal relationships that could have appeared to influence the work reported in this paper.

Data availability

The model code is in supplementary. Data are extracted from published papers.

Acknowledgements

We thank Ryne Thomas for his excellent skills in creating plots for this manuscript, and Drs. Eva McLanahan and Miao Li for reviewing this manuscript.

Author credits

JF and CH were responsible for the code. MM performed code review. AN edited the manuscript. DM and MG assisted in the correct interpretation of perchlorate data and thyroid axis perturbations.

Appendix A. Supplementary data

Supplementary data to this article can be found online at https://doi.org/10.1016/j.taap.2023.116733. The perchlorate model parameters and model code (csl) are provided.

References

Bianco, A.C., 2022. T3 levels and thyroid hormone signaling. Front. Endocrinol. 13, 1044691. https://doi.org/10.3389/fendo.2022.1044691.

Buckalew, A.R., Wang, J., Murr, A.S., et al., 2020. Evaluation of potential sodium-iodide symporter (NIS) inhibitors using a secondary Fischer rat thyroid follicular cell (FRTL-5) radioactive iodide uptake (RAIU) assay. Arch. Toxicol. 94 (3), 873–885.

Campbell, J.L., Narayanan, L., Ferguson, D.C., Mumtaz, M., El-Masri, H., Fisher, J., 2004. Effect of perchlorate on displacement of thyroxine from serum binding proteins and binding of perchlorate to serum proteins. In: Vol Abstract #1366. The Toxicologist, A supplement of Toxicological Sciences.

Clewell, R.A., Merrill, E.A., Yu, K.O., et al., 2003. Predicting fetal perchlorate dose and inhibition of iodide kinetics during gestation: a physiologically-based pharmacokinetic analysis of perchlorate and iodide kinetics in the rat. Toxicol. Sci. 73 (2), 235–255.

Crofton, K.M., 2004. Developmental disruption of thyroid hormone: correlations with hearing dysfunction in rats. Risk Anal. 24 (6), 1665–1671. https://doi.org/10.1111/j.0272-4332.2004.00557.x.

Dai, G., Levy, O., Carrasco, N., 1996. Cloning and characterization of the thyroid iodide transporter. Nature 379 (6564), 458–460.

D'angelo, S., Paul, D., Wall, N., Lombardi, D., 1976. Pituitary thyrotropin (TSH) rebound phenomenon and kinetics of secretion in the goitrous rat: differential effects of thyroxine on synthesis and release of TSH. Endocrinology 99 (4), 935–943.

De Escobar, G.M., Calvo, R., Obregón, M.J., Del Ray, F.E., 1990. Contribution of maternal thyroxine to fetal thyroxine pools in normal rats near term. Endocrinology 126 (5), 2765–2767.

Deisenroth, C., Soldatow, V.Y., Ford, J., et al., 2020. Development of an in vitro human thyroid microtissue model for chemical screening. Toxicol. Sci. 174 (1), 63–78.

Fekete, C., Lechan, R.M., 2007. Negative feedback regulation of hypophysiotropic thyrotropin-releasing hormone (TRH) synthesizing neurons: role of neuronal afferents and type 2 deiodinase. Front. Neuroendocrinol. 28 (2–3), 97–114.

Fisher, J.W., Li, S., Crofton, K., et al., 2013. Evaluation of iodide deficiency in the lactating rat and pup using a biologically based dose-response model. Toxicol. Sci. 132 (1), 75–86.

Fliers, E., Alkemade, A., Wiersinga, W.M., Swaab, D.F., 2006. Hypothalamic thyroid hormone feedback in health and disease. Prog. Brain Res. 153, 189–207.

Friedman, K.P., Watt, E.D., Hornung, M.W., et al., 2016. Tiered high-throughput screening approach to identify thyroperoxidase inhibitors within the ToxCast phase I and II chemical libraries. Toxicol. Sci. 151 (1), 160–180.

Gilbert, M.E., 2023. Submitted.

Gilbert, M.E., O'Shaughnessy, K.L., Axelstad, M., 2020. Regulation of thyroid-disrupting chemicals to protect the developing brain. Endocrinology 161 (10), bqaa106.

Gilbert, M.E., Hassan, I., Wood, C., et al., 2022. Gestational exposure to perchlorate in the rat: thyroid hormones in fetal thyroid gland, serum, and brain. Toxicol. Sci. 188 (1), 117–130.

Goede, S.L., 2022. General Review on Mathematical Modeling in the Hypothalamus Pituitary Thyroid System.

Goede, S.L., Leow, M.K.-S., Smit, J.W., Dietrich, J.W., 2014. A novel minimal mathematical model of the hypothalamus–pituitary–thyroid axis validated for individualized clinical applications. Math. Biosci. 249, 1–7.

Griessen, M., Lemarchandberaud, T., 1973. Thyrotropin secretion and metabolism in rats during propylthiouracil treatment. Endocrinology 92 (1), 166–173.

Hallgren, S., Sinjari, T., Håkansson, H., Darnerud, P., 2001. Effects of polybrominated diphenyl ethers (PBDEs) and polychlorinated biphenyls (PCBs) on thyroid hormone and vitamin a levels in rats and mice. Arch. Toxicol. 75, 200–208.

Hallinger, D.R., Murr, A.S., Buckalew, A.R., Simmons, S.O., Stoker, T.E., Laws, S.C., 2017. Development of a screening approach to detect thyroid disrupting chemicals that inhibit the human sodium iodide symporter (NIS). Toxicol. in Vitro 40, 66–78.
Jing, L., Zhang, Q., 2022. Intrathyroidal feedforward and feedback network regulating thyroid hormone synthesis and secretion. Front. Endocrinol. 13, 992883.
Kosugi, S., Sasaki, N., Hai, N., et al., 1996. Establishment and characterization of a Chinese hamster ovary cell line, CHO-4J, stably expressing a number of Na+/I− symporters. Biochem. Biophys. Res. Commun. 227 (1), 94–101.
Lu, M.-H., Anderson, R.R., 1994. Thyroxine secretion rates during pregnancy in the rat. Endocr. Res. 20 (4), 343–364.
Lumen, A., Mattie, D.R., Fisher, J.W., 2013. Evaluation of perturbations in serum thyroid hormones during human pregnancy due to dietary iodide and perchlorate exposure using a biologically based dose-response model. Toxicol. Sci. 133 (2), 320–341.
Mahle, D.A., Yu, K.O., Narayanan, L., Mattie, D.R., Fisher, J.W., 2003. Changes in cross-fostered Sprague-Dawley rat litters exposed to perchlorate. Int. J. Toxicol. 22 (2), 87–94.
McLanahan, E.D., Andersen, M.E., Fisher, J.W., 2008. A biologically based dose-response model for dietary iodide and the hypothalamic-pituitary-thyroid axis in the adult rat: evaluation of iodide deficiency. Toxicol. Sci. 102 (2), 241–253.
Merrill, E.A., Clewell, R.A., Gearhart, J.M., et al., 2003. PBPK predictions of perchlorate distribution and its effect on thyroid uptake of radioiodide in the male rat. Toxicol. Sci. 73 (2), 256–269.
Merrill, E.A., Clewell, R.A., Robinson, P.J., et al., 2005. PBPK model for radioactive iodide and perchlorate kinetics and perchlorate-induced inhibition of iodide uptake in humans. Toxicol. Sci. 83 (1), 25–43.
Miller, M.D., Crofton, K.M., Rice, D.C., Zoeller, R.T., 2009. Thyroid-disrupting chemicals: interpreting upstream biomarkers of adverse outcomes. Environ. Health Perspect. 117 (7), 1033–1041.
Nadel, A.S., Ballermann, B.J., Anderson, S., Brenner, B., 1988. Interrelationships among atrial peptides, renin, and blood volume in pregnant rats. Am. J. Phys. Regul. Integr. Comp. Phys. 254 (5), R793–R800.
Olker, J.H., Korte, J.J., Denny, J.S., et al., 2019. Screening the ToxCast phase 1, phase 2, and e1k chemical libraries for inhibitors of iodothyronine deiodinases. Toxicol. Sci. 168 (2), 430–442.
Ramhøj, L., Svingen, T., Mandrup, K., Hass, U., Lund, S.P., Vinggaard, A.M., Hougaard, K. S., Axelstad, M., 2022. Developmental exposure to the brominated flame retardant DE-71 reduces serum thyroid hormones in rats without hypothalamic-pituitary-thyroid axis activation or neurobehavioral changes in offspring. PLoS One 17 (7), e0271614. https://doi.org/10.1371/journal.pone.0271614.
Ramhøj, L., Axelstad, M., Baert, Y., et al., 2023. New approach methods to improve human health risk assessment of thyroid hormone system disruption–a PARC project. Front. Toxicol. 5, 1189303.
Rivard, L.A., 2007. Determining the Affinity of Perchlorate for Proteins in Rat Serum Using Equilibrium dialysis and Ion Chromatography. University of Georgia, Undergraduate Honors.
Rodríguez-Rodríguez, A., Lazcano, I., Sánchez-Jaramillo, E., et al., 2019. Tanycytes and the control of thyrotropin-releasing hormone flux into portal capillaries. Front. Endocrinol. 10, 401.
Rolland, N.C., Bothe, K., Schorsch, K., Sheets, L., Zorrilla, L., Blanck, O., 2023. Establishment of a qAOP to Describe Thyroid Disruption Leading to Neurodevelopmental Toxicity in Rat. Paper presented at the Society of Toxicology, Nashville TN.
Schlosser, P.M., 2016. Revision of the affinity constant for perchlorate binding to the sodium-iodide symporter based on in vitro and human in vivo data. J. Appl. Toxicol. 36 (12), 1531–1535.
Versloot, P., Van der Heide, D., Schroeder-Van Der Elst, J., Boogerd, L., 1998. Maternal thyroxine and 3, 5, 3′-tri-iodothyronine kinetics in near-term pregnant rats at two different levels of hypothyroidism. Eur. J. Endocrinol. 138 (1), 113–119.
Wang, J., Hallinger, D.R., Murr, A.S., et al., 2018. High-throughput screening and quantitative chemical ranking for sodium-iodide symporter inhibitors in ToxCast phase I chemical library. Environ. Sci. Technol. 52 (9), 5417–5426.
WHO IPoC, 2010. Characterization and Application of Physiologically Based Pharmacokinetic Models in Risk Assessment. World Health Organization Geneva, Switzerland.
Wolff, J., Walrey, J., 1963. Thyroidal iodide transport: IV. The role of ion size. Biochim. Biophys. Acta 69, 58–67.
Yoon, M., Nong, A., Clewell III, H.J., Taylor, M.D., Dorman, D.C., Andersen, M.E., 2009. Evaluating placental transfer and tissue concentrations of manganese in the pregnant rat and fetuses after inhalation exposures with a PBPK model. Toxicol. Sci. 112 (1), 44–58.
York, R.G., Funk, K.A., Girard, M.F., Mattie, D., Strawson, J.E., 2003. Oral (drinking water) developmental toxicity study of ammonium perchlorate in Sprague-Dawley rats. Int. J. Toxicol. 22 (6), 453–464.
Yu, K.O., Narayanan, L., Mattie, D.R., et al., 2002. The pharmacokinetics of perchlorate and its effect on the hypothalamus–pituitary–thyroid Axis in the male rat. Toxicol. Appl. Pharmacol. 182 (2), 148–159. https://doi.org/10.1006/taap.2002.9432.
Zhang, X., Kellogg, A.P., Citterio, C.E., et al., 2021. Thyroid hormone synthesis continues despite biallelic thyroglobulin mutation with cell death. JCI Insight 6 (11).
Zoeller, R.T., 2007. Environmental chemicals impacting the thyroid: targets and consequences. Thyroid 17 (9), 811–817.